Vol 13 No 1, January 2004
1009-1963/2004/13(01)/0019-05

Chinese Physics

© 2004 Chin. Phys. Soc.
and IOP Publishing Ltd

# Research on high-$T_c$ SQUID based non-destructive evaluation*

Wang Hui-Wu(王会武), Kong Xiang-Yan(孔祥燕), Ren Yu-Feng(任育峰), Yu Hong-Wei(于洪伟), Ding Hong-Sheng(丁红胜), Zhao Shi-Ping( 赵士平), Chen Geng-Hua(陈赓华)†, Zhou Yue-Liang(周岳亮), Zhang Li-Hua(张利华), He Yu-Sheng(何豫生), and Yang Qian-Sheng(杨乾声)

*Institute of Physics, Chinese Academy of Sciences, Beijing* 100080, *China*

(Received 6 June 2003; revised manuscript received 23 July 2003)

A non-destructive evaluation system based on high-$T_c$ dc-SQUID (superconducting quantum interference device) incorporating a gradient field excitation has been built. By using this system a 1mm-diameter hole at a depth of 2mm inside an aluminium plate at room temperature can be easily detected and imaged in an unshielded environment. The relation between the spatial resolution, or the smallest detectable flaw size, and experimental parameters is briefly analysed in terms of a simple metal ring model. The result shows that the spatial resolution depends strongly on the sensor-sample separation as well as on some other parameters, such as signal-to-noise ratio of excitation, excitation frequency and material conductivity.

**Keywords:** SQUID, resolution, eddy current
**PACC:** 0755, 8170E, 0670D

## 1. Introduction

Non-destructive electromagnetic testing (NDET) based on probing electrical conductivity and/or magnetic permeability of materials with magnetic or electric sensors is one of the most common techniques in material evaluations. The most frequently used conventional magnetic field sensors in NDET, such as Hall probes and magnetoresistors, are still in use and improvement.[1] Such sensors have a higher reproducibility in fabrication of the single sensor and are easier to scale up to form robust sensor arrays.

Recently, superconducting quantum interference devices (SQUIDs) as magnetic field sensors for NDET have revealed their advantages in very high field sensitivity, wide bandwidth, broad dynamic range and excellent linearity.[2−4] Especially, it has been recognized that their extremely high sensitivity makes them very suitable for the detection of deep flaws.[5−7]

Now SQUID based eddy current NDET techniques are commonly used for the detection of hidden defects in nonmagnetic metallic materials. In this technique an excitation coil generates a relatively small alternating magnetic field. This field induces eddy currents in the sample being tested. The currents are deviated by any local flaws and local shape variation within a small scanning area of the sample. The resulting field distortions due to the current deviation are then detected by the SQUID sensors. Obviously, with a small excitation, the evaluation is completely non-invasive.

Typical field excitations for the SQUID based NDET are absolute excitation or differential excitation generated by single or double-D shaped coils respectively.[8,9] Different coil geometries result in different eddy current distributions, as well as corresponding flaw responses. Generally, the sensitivity of NDET depends largely on the excitation–detection schemes.

In this paper, we report a high-$T_c$ dc-SQUID based NDET system incorporating a gradient field excitation and some results of detecting flaws in nonmagnetic conductive plates by using this system. A

*Project supported by the Foundation from the Ministry of Science and Technology of China, and the National Center for R & D on Superconductivity (Grant Nos NKBRSF-G19990646 and 2002AA306412).
†Corresponding author. E-mail: gchen@aphy.iphy.ac.cn

hole as small as 1mm in diameter and 2mm deep inside an aluminium plate at room temperature can be easily detected and imaged with a spatial resolution of 200$\mu$m in unshielded environment. In addition, the spatial resolution for shallow flaw detections, which are useful for plate shaped samples, is analysed and discussed with a simple model.

## 2. Experimental setup

Our SQUID based NDET system consists of a single channel high-$T_c$ SQUID magnetometer, a liquid nitrogen Dewar, a sample stage and a control unit. This system together with the specially developed sensor electronics allows the detection of magnetic impurities or the measurement of eddy current field.

A YBCO dc-SQUID is mounted in vacuum on the end of a cold finger fixed at the inner wall bottom of the Dewar, which is filled with liquid nitrogen (77K) to cool the SQUID sensor. The sensor faces a thin flat sapphire window on the outer wall of the Dewar and is thermally isolated from it by a vacuum space in a distance of less than 1mm. [10]

A plate-shaped sample is placed outside the window on a movable stage with a scanning area up to 50mm×50mm and a positioning accuracy reaching the $\mu$m range.

To contribute as little as possible to the sample–sensor distance, it is essential that on the one hand the window must be as thin as possible and on the other hand that it also must be relatively small in diameter, in order to limit the concavely bending of the window under atmosphere pressure. By using a window with a thickness of 80$\mu$m and a diameter of 7mm, a sample–sensor distance of less than 2mm can be obtained in our measurements.

We use a double-D shaped coil adhered to the bottom of the sample to generate an alternating differential excitation. The plane of the coil is parallel to that of the SQUID. The horizontal position of the coil is well adjusted to balance the excitation flux and thus eliminates the direct signal detected by the sensor.

We use a directly coupled YBCO thin film dc-SQUID sensor with a loop inductance of 60 pH and a washer area of 400$\mu$m × 400$\mu$m comparable to the range of sample–sensor distance. The background flux noise level is about $1.3 \times 10^{-3}$ $\Phi_0/\mathrm{Hz}^{1/2}$ at 10Hz, which is more than one order of magnitude larger than the intrinsic flux noise. The SQUID sensor is connected to room temperature flux locked loop (FLL) electronics via a matching circuit at liquid nitrogen temperature. A magnetic field signal due to eddy current deviation detected by the SQUID sensor is magnified by the FLL and then processed via a narrow band lock-in readout unit with a central frequency of 710Hz and bandwidth of 7Hz.

When the test sample is uniform within the excitation area, the eddy current is symmetrical and its magnetic field anti-symmetrical with respect to the central plane of the sensor–excitation complex. In this case we have no response signal except noise. When a flaw in the test sample is scanned in or out of the excitation area, the symmetry of the field distribution is broken. The asymmetrical magnetic field was generated and may be detected.

## 3. Results

Firstly, in order to calibrate the magnetic field and the sample–sensor distance of the instrument before testing, we imaged the magnetic field distribution generated by a current dipole. Figure 1(a) shows the scheme for calibration. The dipole with a strength of $I \cdot \mathrm{d}l = 2\mu\mathrm{A{\cdot}m}$ is placed in parallel with the SQUID plane on the sample stage and its field distribution of $z$-component in the measuring plane is recorded by scanning the sample stage in $x$- and $y$-directions. Figure 1(b) shows the measured field distribution map in two-dimensional (2D) form consisting of 6400 data points, which cover an area of 9.6mm×9.6mm. The dwelling time of data taking for each point is 200ms. The map has two poles as expected, a maximum and a minimum, corresponding to the field of $\pm B_z^{\max}$. Thus, the distance $\Delta$ between the two poles is also given. From dipole field expression, the $z$-component of the maximum field is

$$B_z^{\max} = \mu_0 I \cdot \mathrm{d}l / 3\sqrt{3}\pi\Delta^2, \tag{1}$$

and the distance between the dipole (sample) and sensor can be simply written as

$$d = \Delta/\sqrt{2}, \tag{2}$$

where $\mu_0$ is the vacuum permeability, $I \cdot \mathrm{d}l$ is the strength of the current dipole. From $\Delta$=2mm, we obtain $B_z^{\max}$=38nT and $d$=1.4mm.

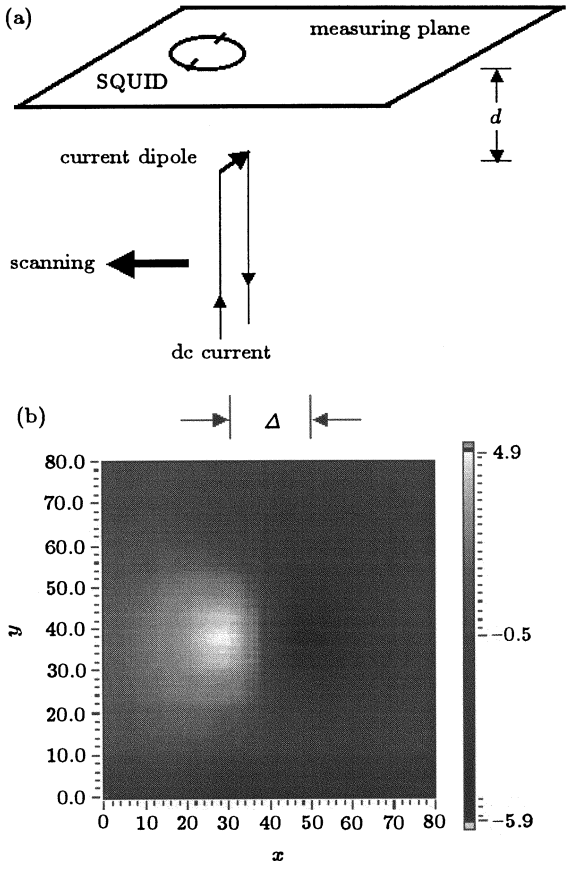



**Fig.1.** (a) Schematic for magnetic field calibration with a current dipole below the measuring plane at a distance of $d$. When the dipole scans in $x$- and $y$-directions on the sample stage, the SQUID in the measuring plane records the magnetic field produced by the dipole. (b) The 2D-form distribution map of $z$-component of the magnetic field measured in the SQUID plane. It consists of 80 × 80 data points. The distance between adjacent two points in each direction is 120$\mu$m and the whole map covers 9.6mm×9.6mm. The right side bar marks the magnetic field scale in arbitrary units.

The operation of the instrument has been demonstrated by testing a pile of three 2mm thick aluminium plates fixed in parallel with the SQUID plane. There is a 0.8mm wide slot in the middle plate of the triple plate pile.

A planar double-D shaped coil is mounted at the bottom of the plates. An excitation current with a magnitude up to 10mA is applied to the coil to generate a planar magnetic field gradient.

The penetration depth of the excitation field, or the skin depth

$$\delta = \sqrt{2/\mu\sigma\omega} \qquad (3)$$

restricts the depth under the surface of the tested material in which flaws may be found, where $\mu$ is permeability and $\sigma$ conductivity of the material, and $\omega$ is the frequency of the excitation wave. We use a narrow band lock-in detection with a sinusoidal excitation at a frequency of 710Hz, which leads to a skin depth of 3mm for aluminium. Figure 2 shows the 2D in-phase data of detected field in the $z$-direction and its integration along the excitation field gradient. A peak of the integrated curve gives the position of the slot.

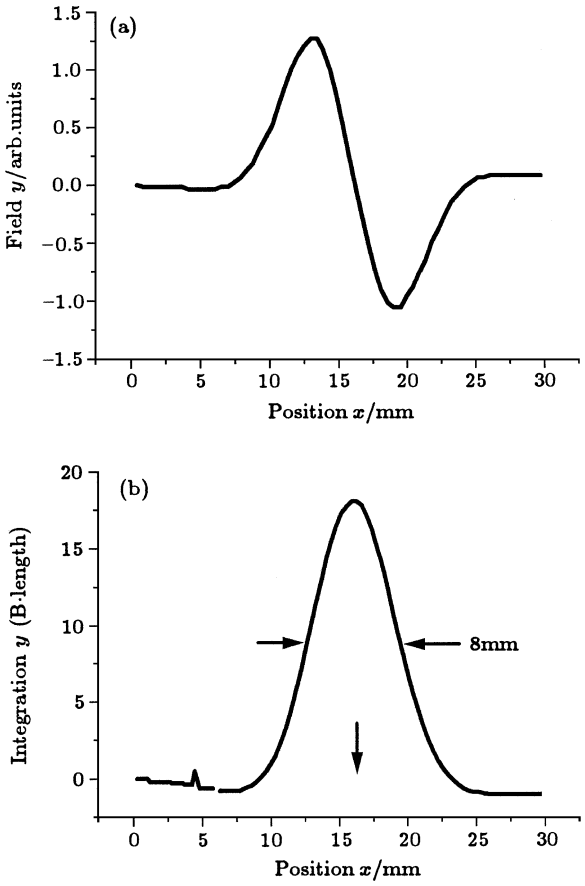



**Fig.2.** (a) The magnetic field data detected for a slot with a width of 0.8mm and (b) its integration along the excitation field gradient. The diameter of the excitation coil is 10mm. The position of the slot centre indicated by an arrow is at the peak in the integration curve.

In another test there is a hole 1mm in diameter in the middle plate, all other testing parameters are the same as above. Figures 3(a) and 3(b) are the resulting field distribution and its integral, respectively, showing an image of the hole with a spatial resolution of about 0.2mm.

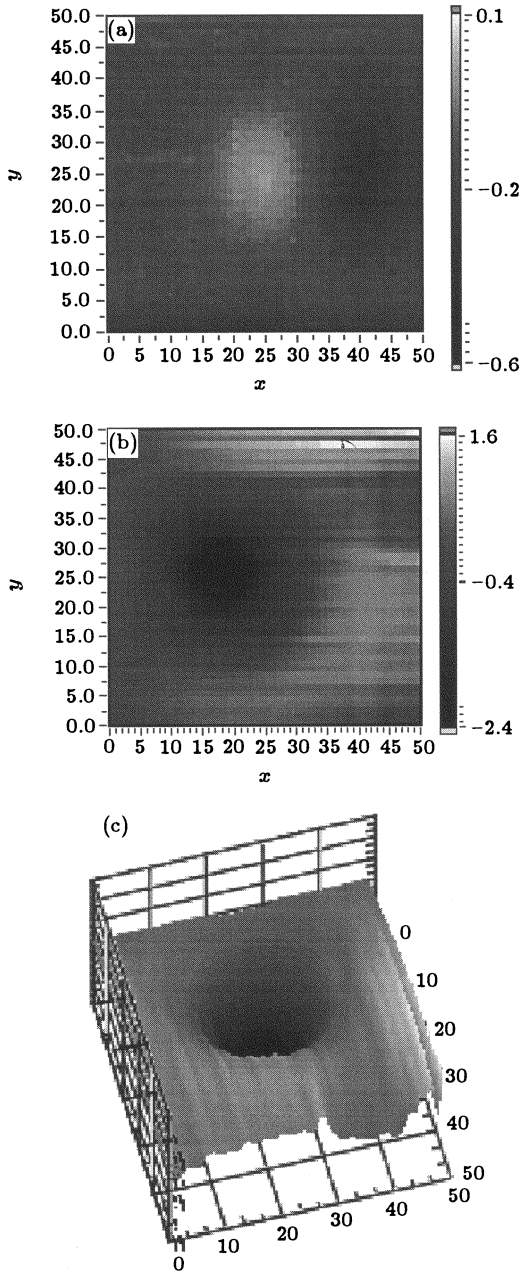



**Fig.3.** (a) The field distribution due to a 1mm-diameter hole at a depth of 2mm inside an aluminium plate and its integration signals along the $x$-axis in (b) 2D and (c) 3D forms. The diameter of the excitation double-D shaped coil is 6mm. Each map consists of 50 × 50 points with 180$\mu$m per step, which covers a scanning area of 9mm × 9mm. The right side bar in (a) and (b) marks the magnetic field scale in arbitrary units.

# 4. Discussion

In practical applications, it is often to detect the flaws in plate-shaped sample, which may be approximately described by shallow flaws with a depth in a few mm range. In order to briefly estimate the smallest detectable size of such flaws, we present a simple model by taking a small metal wire ring instead of metal plate with a small flaw or hole in it. We assume a metal wire ring placed in parallel with the SQUID sensor at a distance $d$ in excitation field $B(x,t)$ in the $z$-direction. The radius and the cross section of the ring and conductivity of the ring material are $a, s$ and $\sigma$, respectively, with $s = \pi a^2$. The magnetic flux $\Phi$ through the ring is

$$\Phi = B(x,t) \cdot \pi a^2. \tag{4}$$

Here we simply use the field at the centre of the ring $B(x,t)$ as the average field in the ring area. In our model the field $B(x,t)$ is produced by an alternating current flowing in the double-D shaped coils. We also assume that the $x$-axis is placed in line with the field gradient of the excitation and its zero point is at the intersection of the sensor-excitation coaxial line and the ring plane. Obviously, at the origin $x$=0, we have $\Phi$=0. In the vicinity of $x$=0, the excitation field is given by

$$B(x,t) = b_0 x \cos(\omega t), \tag{5}$$

where $b_0$ is the amplitude of the field gradient near the origin, $\omega$ is the excitation frequency. Field $B(x,t)$ is a function of time and the ring coordinate in the $x$-axis. When the ring shifts from $x$=0, we have a linear response of flux $\Phi$, and according to the Faraday's law, the EMF along the circle of the ring is

$$\varepsilon = -\mathrm{d}\Phi/\mathrm{d}t = -\pi a^2 \mathrm{d}B(t)/\mathrm{d}t = \pi a^2 x \omega b_0 \sin(\omega t). \tag{6}$$

Considering the ring resistance $R = 2\pi a/(\sigma \pi a^2)$, we obtain the circular eddy current

$$I = \varepsilon/R = (\pi/2) a^3 x \sigma \omega b_0 \sin(\omega t). \tag{7}$$

The $z$-component of magnetic field $B_z$ at the sensor position induced by the current $I$ can be written as

$$B_z = \mu_0 I a^2 / 2(d^2 + a^2)^{3/2}. \tag{8}$$

In $a \ll d$ limit we have

$$B_z = \mu_0 \pi a^5 x \sigma \omega b_0 \sin(\omega t)/4d^3. \tag{9}$$

When the ring is at the coaxial position in the antisymmetric excitation field, there is no circular eddy current flowing around, and the sensor receives no signal except noise. When the ring is scanned with a displacement in the $x$-direction, the induced field $B_z$ is generated. As soon as the averaged field signal, $B_z/\sqrt{2}$, becomes comparable to the noise of the excitation $\delta B_{\mathrm{ex}}$ at the sensor position, the signal can be

just detected by the SQUID sensor and read out by the lock-in amplifier. The radius of the ring, $a$, is supposed to be chosen in such a way that it is equal to the least displacement, that is $x = a$, in which the signal becomes detectable, that is

$$a = \{4\sqrt{2}d^3/[\mu_0\pi\omega\sigma(b_0/\delta B_{\rm ex})]\}^{1/6}. \qquad (10)$$

In this case the radius $a$ may be used as a measure of spatial resolution. Substituting our experimental parameters $d$=1.4mm, $\omega/2\pi$=710Hz, $\sigma$=4 $\times 10^7 \Omega^{-1}{\rm m}^{-1}$ and $b_0/\ \delta B_{\rm ex} = 3.4 \times 10^4 {\rm mm}^{-1}$ at a bandwidth of 7Hz into Eq.(10), we gain $a$=0.29mm, which is close to our experimental result in Fig.3.

Equation (10) shows that the spatial resolution for shallow flaw detection is related to the sample–sensor distance $d$, the excitation frequency $\omega$, conductivity $\sigma$ of the material and the gradient field signal-to-noise ratio ($b_0/\ \delta B_{\rm ex}$), where $b_0$ is the field gradient of excitation at the sample position and $\delta B_{\rm ex}$ is the excitation noise at the sensor position. Generally, the total noise in NDET is dominated by that of the excitation, and it is demanded that the excitation field gradient is high. In order to achieve a fine spatial resolution, it is effective to reduce the distance $d$, including window thickness, window bending, and keep the SQUID sensor and the sample as close as possible to the window without touching it. In addition, an exact balance of the gradient excitation is essential.

Increasing the excitation frequency will not help very much, as it is restricted by the skin depth. In addition, one can use a narrow band lock-in detection to improve the signal to noise ratio, but accordingly one has to take longer time in measurement.

## 5. Conclusions

Eddy current nondestructive tests on aluminium multiplate structures have been performed by using a high-$T_c$ SQUID based system in an unshielded environment. The flaws in a size of 1mm range and as deep as 2mm can be sensitively detected and imaged with the help of a gradient field excitation.

For estimating the spatial resolution, or the smallest detectable size of flaws, we have analysed the effects of some experimental parameters with a simple metal ring model. The results obtained from both experiments and model analyses indicate that the spatial resolution better than 300$\mu$m can be obtained in our gradient excitation–sensor and narrow band lock-in detection schemes.

The expression of the spatial resolution may be useful for quantitative estimation for the smallest detectable size of shallow flaws in NDET.

## References


[1] Seidel P, Dorrer L, Schmidl F, Wunderlich S, Linzen S, Neubert R, Ukhansky N and Goudochnikov S 2000 *Supercond. Sci. Technol.* **13** 537

[2] Weinstock H 1991 *IEEE Trans. Magn.* **27** 3231

[3] Wikswo J P Jr 1995 *IEEE Trans. Appl. Supercond.* **5** 74

[4] Podney W N 1993 *IEEE Trans. Appl. Supercond.* **3** 1914

[5] Muck M, Kreutzbruck M V, Baby U, Troll J and Heiden C 1997 *Physica* C **282** 407

[6] Jenks W G, Sadeghi S S H and Wikswo J P 1997 *J. Phys.* D **30** 293

[7] Kreutzbruck M V, Troll J, Muck M and Heiden C 1997 *IEEE Trans. Appl. Supercond.* **7** 3279

[8] Braginski A I and Krause H J 2000 *Physica* C **335** 179

[9] Kreutzbruck M V, Baby U, Thesis A, Muck M and Heiden C 1999 *IEEE Trans. Appl. Supercond.* **9** 3805

[10] Ding H S, Zhang F H, Yan X M, Han S J, Dong S Y, Yu H W, Chen G H and He Y S 2002 *Chin. Phys.* **11** 1135